JOURNAL OF NANO- AND ELECTRONIC PHYSICS
Vol. **9** No 6, 06002(5pp) (2017)

ЖУРНАЛ НАНО- ТА ЕЛЕКТРОННОЇ ФІЗИКИ
Том **9** № 6, 06002(5cc) (2017)

Electrical Performance of Zinc Oxide Thin Films Transistors

R. Ondo-Ndong, H. Essone-Obame, N. Koumba

Laboratoire pluridisciplinaire des sciences, Ecole Normale Supérieure, B.P 17009 Libreville, Gabon

(Received 15 August 2017; revised manuscript received 15 November 2017; published online 24 November 2017)

The capacitive properties and performance of ZnO (TFT) thin film transistors prepared at 100°C were studied. The ZnO thin films were deposited by rf magnetron sputtering on silicon substrates. The frequency dependence of the conductivity and the capacity of the ZnO thin films was studied in the frequency range from 5 kHz to 13 MHz. Shown that total conductivity increases with frequency and decreases with temperature. This shows that the thermally activated conduction mechanism maintains the correlated barrier of the charge carrier on the localized states as a function of the experimental data. Activation energy is in the range of literature. ZnO-based transistors (TFTs) show non-linearities in both the current voltage and the transfer characteristics which are explained due to the presence of trap states. These traps cause a reversible threshold voltage change as revealed by low frequency capacitance voltage measurements in metal insulating semiconductor (MIS) capacitors. Thermal degradation experiments in heterojunctions confirm the presence of a trap state at 0.32 eV.

Keywords: Thin film transistors, Properties capacities, MIS, ZnO.

DOI: 10.21272/jnep.9(6).06002 PACS numbers: 73.40. – c, 73.50. – h

1. INTRODUCTION

As the thicknesses of several nanometers are narrowed, silicate oxides which carry contemporary MOS components, indispensable quantum-mechanical currents through the gate oxide film severely interfere with the operation of the Component. Materials with high dielectric constant have been considered as potential substitutes for silicon oxide. Compared to the low dielectric permittivity, more charge is induced for the same gate voltage applied. As a result, they can be thicker, which would reduce tunnel currents. As a result, ZnO has a dielectric constant of 8.8 versus 3.9 for SiO_2 [1]. In addition, polycrystalline ZnO has been found for many interesting applications, such as piezoelectric transducers and transparent conductive films, due to many useful properties, such as high mobility, large exciton binding energy, and good transparency [2-6]. Although ZnO-based electronics is promising, there are still many disadvantages that prevent a successful introduction to the market, namely the stability of the device in the presence of atmospheric agents and other adverse effects Caused by the presence of deep traps. Indeed, there have been many reports on native point defects in ZnO, for example, interstitial zinc, interstitial oxygen, and oxygen vacancy. These defects can be the reason for the low quality of ZnO. It is necessary to develop a growth method which can decrease the native point defects in ZnO. At present the main objective of the research to develop new materials for transparent conductivity oxide films consist in obtaining a higher transmittance and a lower resistivity in the visible range of the spectrum. Recently a combination of dielectrics, semiconductors and metal has been used to produce transparent conductive oxides [7-10]. The purpose of this work is to study the capacitive properties and the associated loads, both in the material and at the interface with other materials. ZnO thin films were deposited by rf magnetron sputtering on silicon substrates. The advantage of sputtering is that it can deposit uniform films over a large area. Thermally oxidized silicon substrates have been used for the fabrication of fully transparent thin film transistor (TFT) devices and MIS capacitors. TFT should show good turn-off behavior as well as high mobility. Mobility always increases as the film thickness increases, but it is difficult to achieve good turn-off characteristics in a thicker layer TFT. Therefore, there is an optimum thickness for good TFT characteristics.

2. EXPERIMENTAL METHODS

Magnetron sputtering method was used to deposit the ZnO thin films. Indeed, a target of zinc (99.99%) with a diameter of 51 mm and 6 mm of thickness allowed us to realize these deposits. Silicon substrate used is of the p type with orientation (100). The latter were carefully cleaned with organic products. Magnetron sputtering is carried out in a gas/argon mixture atmosphere. Power supply r.f at frequency of 13.56 MHz is supplied to the system. RF power was about 50 W. Argon and oxygen flow rates were monitored using a flowmeter (ASM, AF 2600). The spraying pressure was maintained at 3.35×10^{-3} Torr controlled by a Pirani gauge. Deposition rates ranged from 0.35 to 0.53 μm/hr. The thin films ranging from 50 nm to 200 nm in thickness were deposited on silicon substrates consisting of a heavily doped silicon gate electrode coated with an insulating SiO_2 thin films at 460 nm. Platinum metal electrodes were then deposited on the ZnO film by thermal evaporation through a shadow mask. The channel had width (W) and a length (L) of 4000 μm and 200 μm, respectively. For the heterostructure, ZnO was deposited above the n-doped silicon. After deposition of the zinc oxide, silver dot electrodes were evaporated on the Pt/ZnO/Ti /Pt/Si sample using an electron weapon evaporation system to render the insulating structure Metallic semiconductor useful for electrical measurements. These were carried out in a vacuum chamber evacuated at about 10^{-3} Torr. Measurements of frequency and temperature dependencies of conductivity and capacity were performed

using a laboratory configuration for AC-based electrical test properties. The samples obtained were tested using an alternating current in the frequency range of 5 Hz to 13 MHz (using a capacitance bridge technique) using measurement temperatures of T_p = 30-300 °C, with *A* Hewlett-Packard LF 4192 A impedance analyzer between silver points and the bottom of the Pt electrode. The temperature was measured with a Doric thermometer (Trendicator 400 K/°C).

3. RESULTS AND DISCUSSION

The both frequency and temperature dependence of conductivity provide at least qualitatively the information about the nature of defect centers in disordered systems and thereby a transport model. This approach uses the notion of carrier hopping between localized sites. This type of theory has helped to explain the conduction phenomenon in a large number of crystalline or noncrystalline materials for which the dispersion behavior in terms of angular frequency of the total measured conductivityt is the sum of two contributions: the ac conductivity and dc conductivity.

3.1 Conductivity Measurements

To search existing design models or study an available new design model with required specifications and to establish the topological structure of these models are the first step of the methodology. The goal of this step is to select some of these models for researching their equivalent mechanism skeleton and kinematic chain for developing the new designs. A different mechanism has been proposed to explain the conductivity $\sigma(\omega)$ in chalcogenide glasses [11-13], Scandium oxide [12] and glasses [12], zinc oxide [14], ceramic [15] and cobalt ferrite [16]. This mechanism is based on the classic jump of charge carriers between the states located above a potential barrier. This process usually involves phonons, due to the height of the barrier. Consider W_M as being the energy difference between the ground state of the potential and the ionized (extended) state distant from *R*. Then, *W* the potential barrier height of the coulombian type is given by the relationship [12]:

$$W = W_M - \frac{4e^2}{\pi\varepsilon R}, \tag{1}$$

where *e* is the effective dielectric constant. In the following, only the cases where the jumps between very close sites are the most important were considered.

The correlated barrier hopping (CBH) model [12] is essentially based on the idea of hopping of the charge carriers between the localized sites over a potential barrier W_M:

$$s = 1 - \frac{6k_BT}{W_M - K_BT\ln\left(\frac{1}{\omega\tau}\right)}, \tag{2}$$

where W_M represents the maximum barrier height (the energy expended by an electron to skip from one site to the nearest one).

In the small polaron tunneling (SPT) [17, 18]

$$s = 1 - \frac{4}{\ln\left(\frac{1}{\omega\tau}\right) - \frac{W_{HO}}{K_BT}}, \tag{3}$$

where $W_{HO} = \frac{e^2}{\varepsilon_p r_p}$ is the polaron hopping energy, ε_p the effective dielectric and r_p the polaron radius. According to these relations, we note that for the QMT model, the exponent s is almost independent of the temperature but there is a frequency dispersion, whereas for CBH model, the value of s is rather less dependent on the frequency but temperature-dependent. By against, for the SPT models increases as *T* increases.

The measurements of conductivity as a function of temperature can still be exploited by studying the variation $\sigma(\omega)$ versus 1000/T which provides an indications about the transport mechanism. This study can be done with the Arrhenius equation expressed by:

$$\sigma_{ac} = \sigma_0 \exp\left(-\frac{E_{ac}}{K_BT}\right), \tag{4}$$

where σ_0 is the pre-exponential factor and E_{ac} the activation energy for the thermally activated process. Under the action of an electric field applied to a material, the response depends on the type of charge carriers: the electrons for conductors, the ions for ionic conductors, and for insulating material characterized by the local displacements of electrons and the orientation of the dipoles, the response is treated in terms of polarization. Dipolar relaxation in the Debye model is purely a viscous process without elastic restoring force between dipoles (orientation polarization under the alternative electric field. In this model [19] the dielectric function which depends on frequency can be written as:

$$\tilde{\varepsilon}(\omega) = \varepsilon_1(\omega) - j\varepsilon_2(\omega), \tag{5}$$

$\varepsilon_1(\omega)$ and $\varepsilon_2(\omega)$ are respectively the real and imaginary dielectric parts. From these parts, we define the dielectric loss tangent $\tan\delta(\omega)$ which is represented as dissipated energy in a dielectric system (dissipation factor) specially in resonance domain:

$$\tan\delta(\omega) = \frac{\varepsilon_2(\omega)}{\varepsilon_1(\omega)}. \tag{6}$$

The dielectric constant $\varepsilon_1(\omega)$ and the loss $\varepsilon_2(\omega)$ can be evaluated using the following relations:

$$\varepsilon_1(\omega) = \frac{C(\omega)d}{S\varepsilon_0}, \tag{7}$$

$$\varepsilon_2(\omega) = \varepsilon_1(\omega)\tan\delta(\omega), \tag{8}$$

where *C* is the measured sample capacitance and ε_0 the free space permittivity. The loss tangent $\tan\delta(\omega)$ can

be also calculated either by the relation (6) or measured directly throw the phase angle Φ using the same described set-up according the relation: $\tan\delta(\omega) = 90° - \Phi$.

Using the Eqs. (4) and (8), it comes:

$$\sigma_{ac}(\omega) = \varepsilon_0 \omega \varepsilon_2(\omega) = \varepsilon_0 \omega \varepsilon_1(\omega) \tan\delta(\omega). \qquad (9)$$

It is this last relation that we used for the calculation of $\sigma_{ac}(\omega)$ knowing the dispersion of $\varepsilon_1(\omega)$ and $\tan\delta(\omega)$. The frequency dependence of the capacity for the sample grown at 100°C. For different temperatures, Fig. 1. While Fig. 2 shows the frequency dependence of the dielectric losses. The C-F characteristics of the deposited ZnO thin films are shown in Fig. 1.

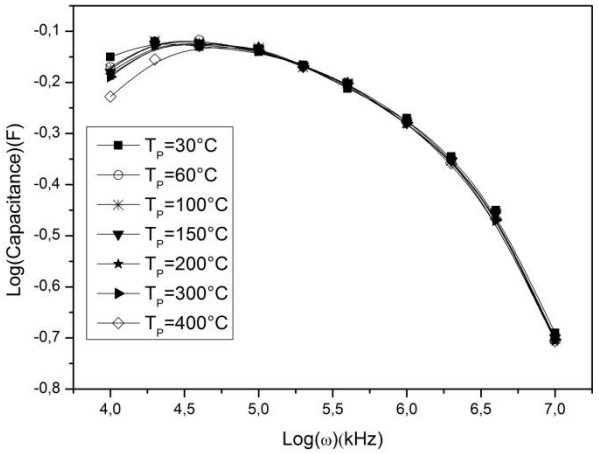

Fig. 1 – The frequency dispersion of capacitance

The capacity at low frequencies is considerably higher than at high frequencies. The capacitance as a function of the frequency has a well-defined plateau in the low Fig. 1, this plate with different capacity values. Indicate the presence of interfacial fault states. The value is constant up to 10^5 Hz is usually labeled C_0 in the literature. This can be explained as follows. Below 10^5 Hz, the interfacial states which are responsible for the transitions between the valence or conduction bands follow the modulation of the applied voltage. Above 10^5 Hz, their response is greatly reduced. The cutoff at 10^7 Hz corresponds to the cut-off frequency RC of the junction. These curves approach the ideal for a ZnO/Si-free defects structure that resembles a straight line with a constant capacity up to the cut-off frequency RC. Our data indicate that interfacial states are partially eliminated. The decrease of the C_0 values with the increase in temperature shows that more fault states are eliminated when the temperature is high while the cut-off frequency remains unchanged.

The results observed in Fig. 2 shows the same behavior as the frequency dependence of the capacitance. We observe, at low temperature, that the dielectric losses are approximately constant as a function of frequency and has a value of the order of 10^{-4}.

At high temperatures, the losses increase with the temperature at low frequencies. The variation of the

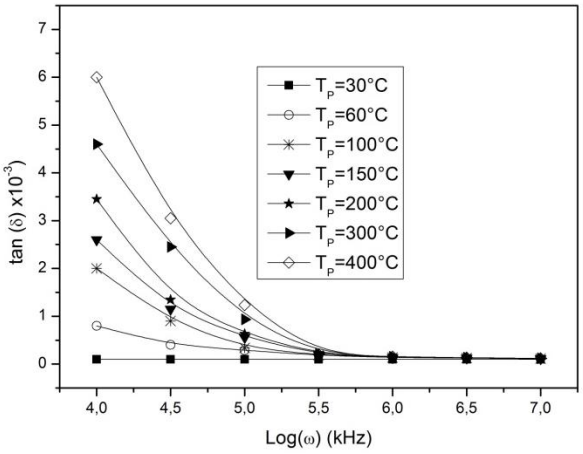

Fig. 2 – The frequency dispersion of $\tan\delta(\omega)$ at different temperatures

capacitance and the dielectric losses as a function of the frequency at different temperatures does not exhibit a relaxation peak. The absence of a relaxation peak in the field of study is due to the fact that dielectric losses are low in our sample. Sign of a good quality sample. Thus, the contribution of the imaginary part to the total permittivity is negligible. The measured *C-V* characteristics of the studied Pt/ZnO/Ti/Pt/Si structures are typical for an MIS structure.

This, in order to obtain more information on the establishment of the accumulation channel as well as on the loads trapped on the ZnO/Si interface. Figs. 3 and 4 illustrate this assertion, wherein the *C-V* characteristics of the MIS structure with ZnO thin films deposited at 100°C at different frequencies and temperatures. The characteristics measured at 10 kHz and 10 MHz clearly revealed the regions of accumulation, depletion and inversion in the *C-V* plots of these figures. The *C-V* parcel of 10 MHz measured at room temperature was moved to more positive voltages than the ideal *C-V*. This offset showed that there was a fixed dielectric fixed charge in the ZnO thin films with a density of the order of 10^{17} cm^{-2}, which has a low tendency to increase with increasing temperature. Bound defects were negatively charged, while the fixed oxide charge was always positive in a ZnO-Si MIS structure. In Fig. 3, it can be seen that by decreasing the measurement frequency, the capacity values become larger in the accumulation, depletion and inversion regions. The 10 kHz *C-V* characteristics showed maximum capacity in the depletion region, while the capacity of the accumulation region increased little. The increase of nearly an order of magnitude with respect to the corresponding capacitance measured at 10 MHz in the depletion region indicates the presence of interface traps at the ZnO-Si interface and of deep Si-levels The increase in capacity in the accumulation region indicates the presence of deep levels in the mass of ZnO thin films which capture and emit charge carriers during voltage scans.

3.2 Transistor Characteristics

The title of the article should concisely and fully describe the content of the article. In the title the following is undesirable.

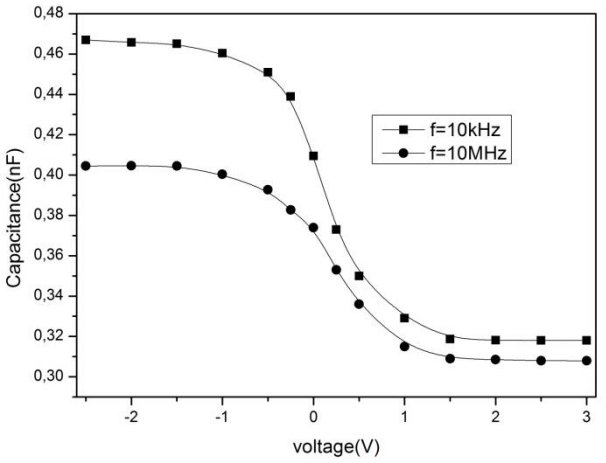

Fig. 3 – *C-V* characteristics of MIS structure with ZnO films dependence of measurement frequency

ZnO thin films were deposited by rf magnetron sputtering on silicon substrates. Thermally oxidized silicon substrates have been used for the fabrication of fully transparent thin film transistors (TFT) and MIS capacitors, see Fig 4.

TFT structures have been used to estimate charge mobility and capacitors have been measured Using low sensitivity impedance techniques to evaluate interface states. TFT shows good deactivation behavior as well as high mobility.

Mobility always increases as the film thickness increases, but it is difficult to get a good trigger characteristics in a thicker TFT. Therefore, there is an optimum thickness for good TFT characteristics. The thin film transistors (TFTs) used in this study have good electrical characteristics with low current, charge mobility of 4.13 cm^2/Vs and modulation ratio 10^4. The I_{DS}-V_{DS} curves of Fig. 5.

Present an n-channel operation, a current saturation and negligible non-linearities in the linear region. Indeed, this TFT operates as an n-channel enhancement mode device, as evident from the fact that a positive gate

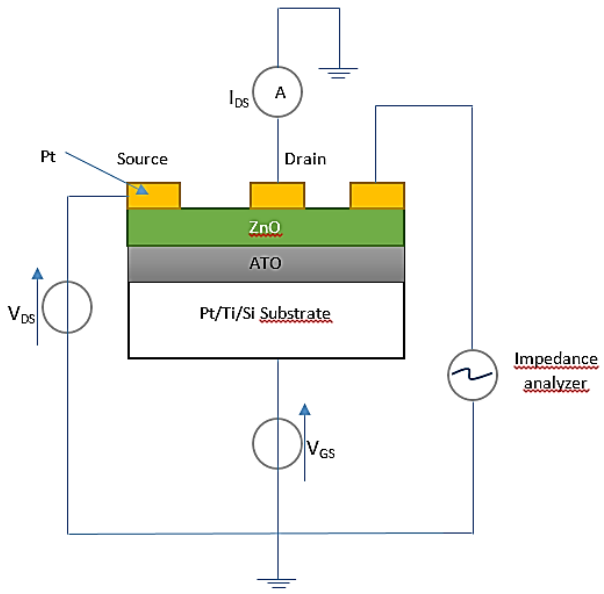

Fig. 4 – Schematic diagram of the device structure

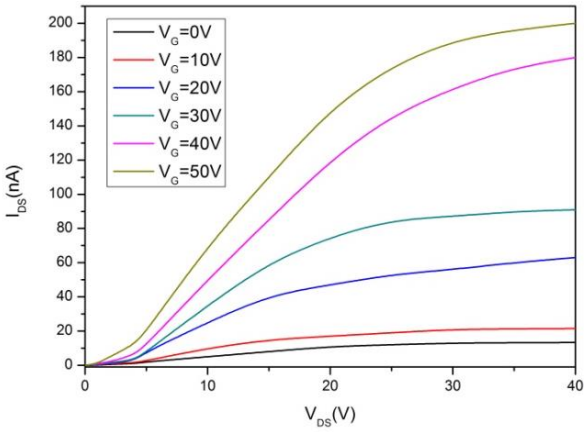

Fig. 5 – Drain current for gate voltages

voltage is required to induce a conducting channel, and that the channel conductivity increases with increasing positive gate bias. Enhancement mode is preferable to depletion mode behavior, in which application of a gate voltage is required to turn the transistor off, since circuit design is easier and power dissipation is minimized when normally-off, enhancement-mode transistors are employed. Second, this device exhibits "hard" saturation, as witnessed by the fact that the slope of each I_{DS} curve is flat for large V_{DS}. Hard saturation indicates that the entire thickness of the ZnO channel can be depleted of free electrons. Hard saturation is highly desirable for most circuit applications, since transistors exhibiting this property possess a large output impedance. The transistor is activated with a film of ZnO having a thickness of about 80 nm. By comparing these characteristics with other ZnO data in the literature, it is important to note that the thickness of the dielectric used is exceptionally large, of the order of 500 nm. If a typical dielectric of 100 nm thickness was used, a similar current modulation with a 20 V gate polarization would be expected. As in many other materials, the transistor transfer characteristics are not linear in a linear plot. Indeed, it is difficult to obtain a single slope and the interception from which the mobility (μ) and the threshold voltage (V_{th}) can be extracted. This problem is well known and has been addressed in a-Si TFT technology [20] as well as in devices based on organic compounds [21]. This behavior occurs when there is a high density of traps relative to the density of free carriers. Particular care is then required when estimating the values of mobility. Usually, load mobility is assumed to increase with the gate voltage such that VGS is the gate-source voltage and ɤ is an empirical parameter defining the variation in mobility with VGS. The drain current in the linear region, ie for a low drain voltage and for $V_{GS} > V_{th}$ is then given by:

$$I_{DS} = k\left(v_{GS} - V_{th}\right)^{1+\gamma} V_{DS}, \qquad (10)$$

with $k = \dfrac{\mu_0 C_0 W}{L}$, μ_0 empirical parameter, C_0 oxide capacity per unit area and the threshold voltage.

The linear transfer curve plotted is shown in Fig 6. The measured drain current at drain-source voltage of 30 V. Obtained mobility at 4.13 $cm^2/Vsec$, 4×10^6 On-off

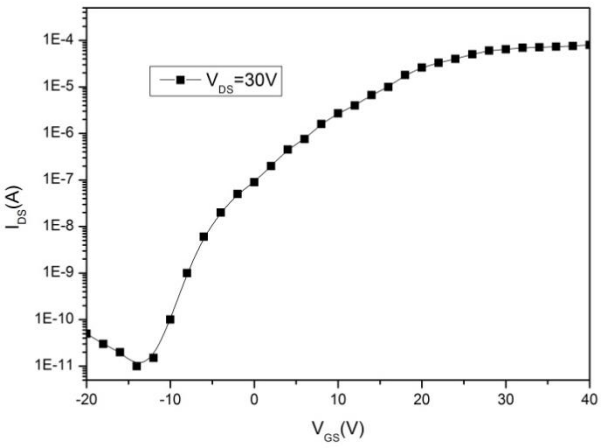

Fig. 6 – Transistor current-voltage characteristics

ratio and threshold voltage of – 6 V. This is an important figure of-merit for AMLCD applications; a ratio of greater about 10^6 is typically required. The gate leakage current magnitude is quite respectable and can be significantly reduced by decreasing the gate area; note that the gate leakage current scales directly with gate area, while the drain current is established by the transistor width-to-length ratio, not by absolute device dimensions. In addition, curves become clearly linear for small, often referred to as contact effects. It can also be explained by the hypothesis of Poole and Frenkel field-assisted field excitation from abundant deep levels. In summary, the characteristics of ZnO TFT show nonlinearities, both in *I-V* and transfer characteristics, both effects are known to be caused by the presence of abundant deep localized levels.

4. CONCLUSSION

The electrical characterization of ZnO thin films in metallic insulating semiconductor structures revealed that the traps strongly affected the electrical characteristics. Indeed, the capacitance and conductivity dependencies were tested for ZnO thin films prepared at a substrate temperature of 100°C. The frequency dependencies of the capacitance and the electrical losses indicate that an appreciable overlap on the Small Polaron Tunnel (SPT). The measured *C-V* characteristics of the Pt/ZnO/Ti/Pt/Si structures studied at 10 kHz and 10 MHz clearly revealed regions of accumulation, depletion and inversion in the plots. This offset showed that there was a fixed dielectric charge in the ZnO thin films with a density of the order of 10^{17} cm^{-2}, and therefore a low tendency to increase with increasing temperature. Particular care is required for the interpretation of TFT parameters and the use of conventional models to extract the parameters of the device such as load mobility. The oxygen content during the deposition of ZnO has a remarkable effect on the conductivity of the thin film by changing the density of the trap. The TFT devices are deposited under a low oxygen content which gives us non-linear *I-V* and transfer characteristics, typical behavior of devices having a high density of trapping states. The mobility of loads is also considerably reduced due to a high density of traps.

REFERENCES

1. C. Casteleiro, H.L. Gomes, P. Stallinga, L. Bentes, R. Ayouchi, R. Schwarz, *J. Non-Cryst. Solids* **354**, 2519 (2008).
2. B.X. Li, Y.F. Wang, *Superlatt. Microstr.* **47** 615 (2010).
3. S.Q. Wei, Y.Y. Chen, Y.Y. Ma, Z.C. Shao, *J. Mol. Catal. A.* **331**, 112 (2010).
4. J. Wang, X.M. Fan, D.Z. Wu, J. Dai, H. Liu, H.R. Liu, Z.W. Zhou, *Appl. Surf. Sci.* **258**, 1797 (2011).
5. L.R. Zheng, Y.H. Zheng, C.Q. Chen, Y.Y. Zhan, X.Y. Lin, Q. Zheng, K.M. Wei, J.F. Zhu, *Inorg. Chem.* **48**, 1819 (2009).
6. T.W. Chen, Y.H. Zheng, J.M. Lin, G.N. Chen, *J. Am. Soc. Mass Spectrom.* **19**, 997 (2008).
7. A. Dhar, T.L. Alford, *APL Materials* **1**, 012102 (2013).
8. X.Y. Liu, Y.A. Li, S. Liu, H.L. Wu, H.N. Cui, *Thin Solid Films*, **520**, 5372 (2012).
9. D.R. Sahu, S.Y. Lin, J.L. Huang, *Appl. Surf. Sci.* **252**, 7509 (2006).
10. D.R. Sahu, J.L. Huang, *Thin Solid Films* **515**, 876 (2006).
11. S.R. Elliott, *Phil. Mag.* **36 (6)**, 1291 (1977).
12. G.E. Pike, *Phys. Rev.* **6**, 1572 (1972).
13. S.R. Elliott, *Solid State Comm.* **27**, 749 (1978).
14. Li-Wen Lai, Ching-Ting Lee, *Mat. Chem. Phys.* **110**, 393 (2008).
15. W.H. Jung, *Cond. Matter* **403**, 636 (2008).
16. N. Sivakumar, A. Narayanasamy, K. Shinoda, C.N. Chinnasamy, B. Jeyadevan, and J.-M. Greneche, *J. Appl. Phys.*, **102**, 013916 (2007).
17. A.R. Long, *Adv. Phys.* **31**, 553 (1982).
18. R.H. Chen, R.Y. Chang, C.S. Shern, T. Fukami, *J. Phys. Chem. Sol.* **64**, 553 (2003).
19. R. Gerhardt, *J. Phys. Chem. Sol.* **55**, 491 (1994).
20. A. Cerdeira, M. Estrada, R. Garcia, A. Oriz-Conde, F.J. Garcia Sanchez, *Solid-State Electronics.* **45**, 1077 (2001).
21. P. Stallinga, H.L. Gomes, F. Biscarini, M. Murgia, D.M. de Leeuw, *J. Appl. Phys.* **96**, 5277 (2004).